

29

TJNAF(CEBAF)

A top priority for the field of nuclear physics in the U.S. since the late 1970's, the Thomas Jefferson National Accelerator Facility (TJNAF) was approved for construction by Congress in 1987. This project was originally called CEBAF, the Continuous Electron Beam Accelerator Facility. It came into operation in Newport News, Virginia, in 1994. The first physics results were reported at the Particles and Nuclei International Conference (PANIC) held at the College of William and Mary in Williamsburg in 1996. The experimental program at TJNAF is now fully underway, and one can look forward to a steady output of significant experimental results providing insight into the structure of hadronic matter well into the 21st century.

Some of the new experimental results from TJNAF have already been referred to in this book, and we discuss more of the anticipated program in the next chapter. In order to fully understand the future opportunities this facility provides, we present a brief overview of the existing accelerator and major experimental equipment.

There is no single feature that makes TJNAF unique; each of the characteristics has been achieved previously at one location or another. Rather, it is the combination of properties that makes TJNAF (CEBAF) the world's most powerful microscope for looking at the nucleus. A schematic of the accelerator complex at TJNAF is shown in Fig. 29.1.

The accelerator itself is in the form of a racetrack 10 m underground. The basic accelerating structure is a superconducting niobium cavity fed with microwave power at a frequency of $\nu = 1497$ MHz. A longitudinal electric field in the cavities accelerates 0.5 mm-long packets of electrons down the linac, which is composed of self-contained cryomodules each containing four cavity pairs. After exiting from the injector, the electrons are moving at close to the velocity of light $c = 2.998 \times 10^{10}$ cm s⁻¹. The wavelength determining the longitudinal cavity dimension is then $\lambda = c/\nu = 20.0$ cm,

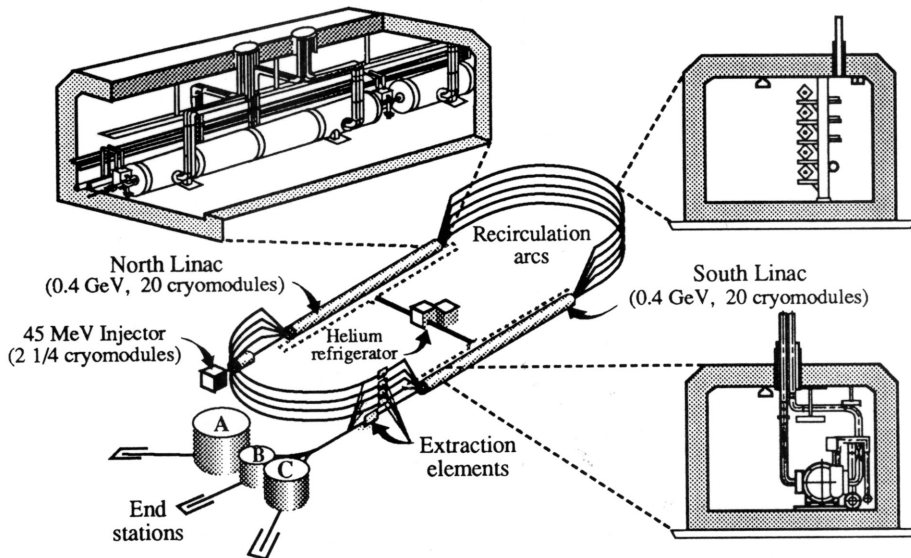


Fig. 29.1. Schematic of the accelerator complex at TJNAF [Le93].

and the period of the field oscillation is $\tau = 1/\nu = 0.668$ ns. The linac accelerates the electrons and increases the energy by 0.4 GeV on the first pass. The electron beam is then extracted from the first linac, passed through its own magnetic return arc, and re-injected into a second linac which adds an additional 0.4 GeV to the energy. The electron packets are again separated, magnetically returned, and re-injected into the first linac. It is a remarkable property of special relativity that even though the electrons may have different *energy*, they are moving with essentially the same *velocity*, namely the velocity of light c . The returned electron bunch can thus be placed spatially on top of a new bunch and accelerated with it. As designed, this process is repeated 5 times, until the electrons reach an energy of 4 GeV.¹ A precise electronic timing system keeps track of the location of each bunch, and on the final pass, the electrons are deflected out of the beam by an RF separator. They are then steered magnetically to one of three independent end stations. The electrons can, of course, be extracted after fewer circuits, to provide a beam of lower energy. In standard operation, every third bunch is steered to a given end station. The time between electron bunches is then $3\tau = 2.00$ ns during which time the electrons go 60.0 cm. At full current, $200 \mu\text{A}$ can be placed on target in each end station. Since the electron bunches come continuously, instead of in the well-separated macropulses of a room-temperature linac which

¹ The field gradient in the CEBAF cavities significantly exceeds design specification, and an accelerator upgrade to 6 GeV has been carried out.

requires recovery time to dissipate the generated heat, one says the beam is continuous; the *duty factor* of the machine is $df = 100\%$. An electron beam polarized at the photo-cathode source can be readily transported through the accelerator and delivered on target. Polarizations as high as $\approx 75\%$ have now been obtained.

Although the cavities are superconducting, there are RF losses in the walls. The accelerating structures are immersed in superfluid ^4He at $\approx 2^\circ\text{K}$ that carries off the generated heat. TJNAF is, in fact, the world's largest superfluid ^4He facility. Focusing magnetic elements keep the beam in line and well inside the machine aperture. The exiting beam has a remarkably low emittance, which means that it exits the machine as a fine pencil and stays that way for however far one wants to transport it on the site. The intrinsic energy resolution in the beam is $\delta E/E \approx 10^{-4}$ which implies that at 4 GeV one can resolve $\delta E \approx 400\text{keV}$ in the target, well suited to the energy scale of nuclear physics. Since not much happens at low temperatures, the beam is remarkably stable once the machine is up and running.

The experimental areas at TJNAF consist of three round halls of wassertank construction that are independently fed by beam, and in which experiments can be carried out in parallel. In electron scattering experiments, it is always necessary to have one magnetic spectrometer to detect the scattered electron and define the virtual quantum of electromagnetic radiation interacting with the target. Since one of the great advantages of TJNAF is the 100% duty factor that allows coincidence experiments, at least one additional detector is required.

In Hall C, as illustrated in Fig. 29.2, there is a high momentum spectrometer (HMS) constructed from three superconducting quadrupoles and a superconducting dipole (QQD). In simplest optical terms, the quadrupoles act as focusing lenses and the dipole as a dispersive prism with which momentum measurements are made. The final particle is observed in the detector hut with an appropriate detector package. The HMS is capable of detecting scattered electrons with momenta up to 6GeV c^{-1} . The momentum resolution is moderate with $\delta p/p \approx 0.05\text{--}0.1\%$. The solid angle acceptance is sizable with $\Delta\Omega \approx 6.7\text{msr}$ and the angular coverage for the scattered electron is $12^\circ\text{--}90^\circ$. Together with the HMS in Hall C, there is a short-orbit spectrometer (SOS) capable of detecting decaying secondaries with a maximum central momentum of 1.5GeV c^{-1} and with $\delta p/p \approx 0.1\%$, $\Delta\Omega \approx 9\text{msr}$, and angular range $12^\circ\text{--}165^\circ$.

In the initial commissioning phase, during the running of experiment E91-13, a brief test of the high momentum and short-orbit spectrometer pair for kaon detection was performed by the Hall C collaboration [HC96] (Fig. 29.3). In this experiment an electron collides with a proton, the nucleus of the element hydrogen, producing an electron and a

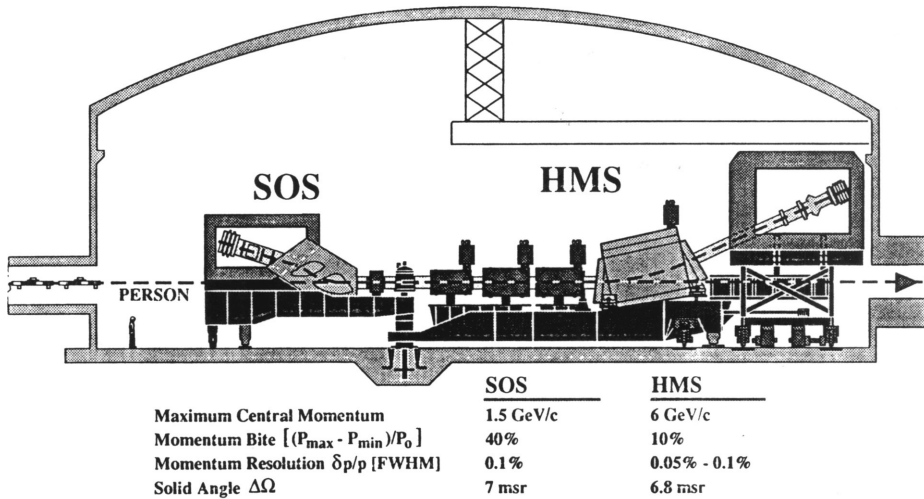


Fig. 29.2. Schematic of major detectors in Hall C at TJNAF [Do93a].

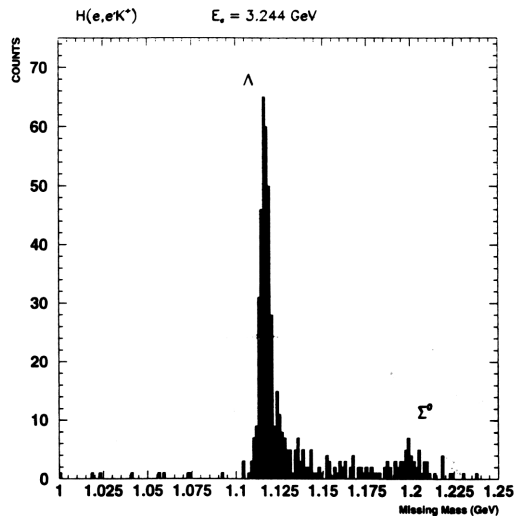


Fig. 29.3. A brief test of the system for kaon detection in $^1\text{H}(e, e' K^+)$ by the Hall C Collaboration during E91-13 at CEBAF [HC96, Wa97].

K^+ meson which are detected in coincidence, along with a variety of other particles which are not detected. In our notation this reaction is $^1\text{H}(e, e' K^+)$. Quarks of positive and negative strangeness are created in pairs in this high-energy reaction, with the K^+ meson being the signature (and the carrier) of the positive strangeness quark. The missing mass (the collective masses of the unobserved particles) spectrum for this reaction,

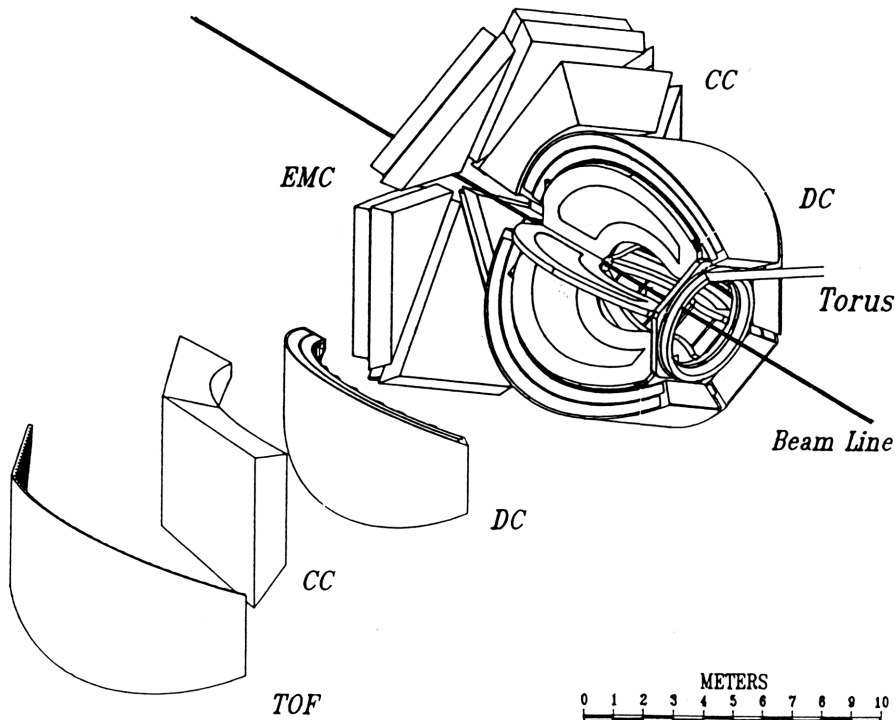


Fig. 29.4. Schematic of CLAS detector in Hall B at TJNAF [Do93a].

shown in Fig. 29.3, is indicative of the effectiveness of the system for kaon electroproduction studies that provide unique access to this process which implants strangeness (through the presence of the strange quarks) into the nucleus. Here the remaining Λ and Σ^0 hyperons produced in this reaction, which now carry negative strangeness, are clearly identified.

The CEBAF Large Acceptance Spectrometer (CLAS) is located in Hall B. This is a device designed to provide maximum coverage for particles emitted in coincidence with the scattered electron. A schematic of this device is shown in Fig. 29.4. Six thin superconducting current coils provide a toroidal field which surrounds the beam axis. Then, like segments of an orange, detector packages are inserted between the coils. The detectors contain drift chambers, Cerenkov counters, and time-of-flight scintillators. An electromagnetic calorimeter of segmented lead glass mounted in the forward direction allows one to detect the scattered electron. While the momentum resolution for the final electron is modest $\delta p/p \approx 1\%$, the detector is able to handle luminosities as high as $10^{34} \text{ cm}^{-2} \text{ s}^{-1}$ and has outstanding particle identification capability for

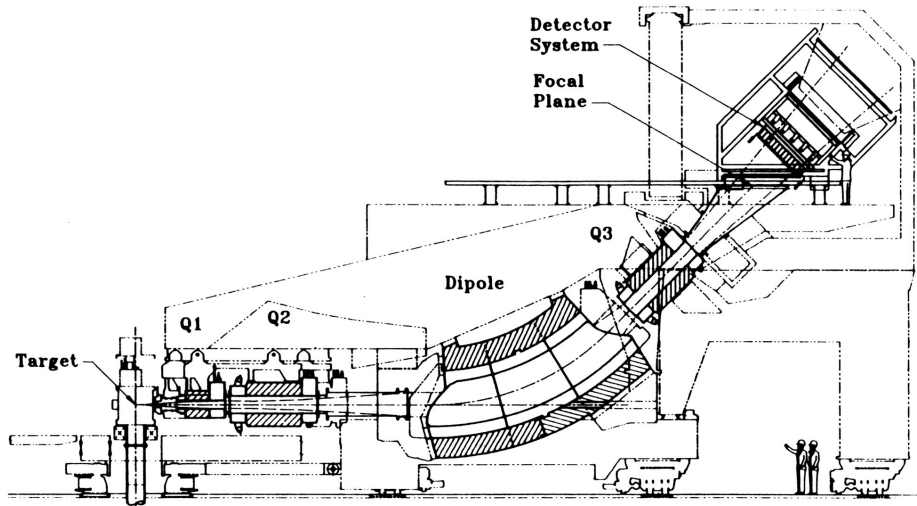


Fig. 29.5. Schematic of HRS detectors in Hall A at TJNAF [Do93a].

single and multiparticle coincidences. An example of some of the initial data from the CLAS detector has already been given in Figs. 28.1 and 28.4.

In Hall A there is a pair of identical high resolution spectrometers (HRS) with properties matched to the outstanding quality of the TJNAF beam itself. The HRS is shown schematically in Fig. 29.5. The HRS is of a QQDQ design, with all magnetic elements superconducting. The momentum range is $0.3\text{--}4.0\text{ GeV } c^{-1}$. The resolution is $\delta p/p \approx 10^{-4}$ and the solid angle coverage is a significant 7 msr . One spectrometer has a detector package for electrons, and the second for hadrons. A polarimeter exists which can be mounted in the hadron arm. The angular coverage of the electron spectrometer is $12.5^\circ\text{--}165^\circ$ and that of the hadron arm is $12.5^\circ\text{--}130^\circ$.

Polarization transfer has been discussed in appendix D. The polarization transfer experiment $^1\text{H}(\vec{e}, e\vec{p})$ measures the product of the magnetic and electric form factors of the proton [Ar81]. Since the magnetic form factor is well known, this interference term allows an accurate determination of G_{Ep} . Figure 29.6 shows one of the first significant experimental results from TJNAF. This is a measurement of G_{Ep}/G_{Mp} [Jo00]. The quality of the data is truly superb. The simplest interpretation of this data is that since the charge form factor falls off faster with Q^2 than the magnetic form factor, the charge density in the proton has a greater spatial extent than the magnetization density. This experiment provides fundamental information on the internal structure of the nucleon.

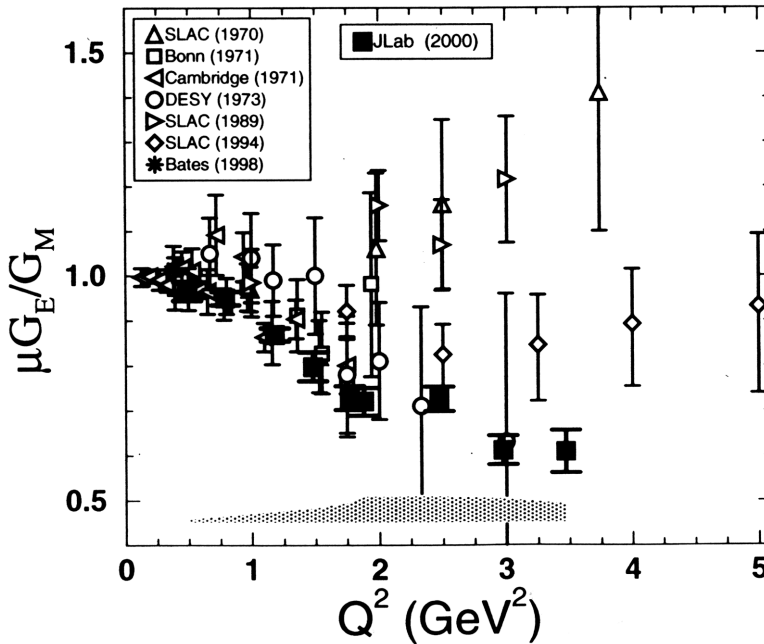


Fig. 29.6. Experimental data on the ratio G_{Ep}/G_{Mp} obtained from polarization transfer measurement $^1\text{H}(\vec{e}, e\vec{p})$ at TJNAF [Jo00]. The author is grateful to C. Perdrisat and M. Jones for the preparation of this figure.

As we have seen in chapter 21, the reaction whereby a polarized electron incident on a nucleus produces a scattered electron and a polarized proton allows one to study how the nucleon spin propagates out from the nuclear interior. In this way one has a direct test of relativistic models of nuclear structure that describe the spin dependence of the nuclear shell model. One of the initial Hall A missing-mass spectra for this reaction on a ^{16}O target producing ^{15}N is shown in Fig. 29.7.

One of the first published experimental papers from TJNAF presents the results from CEBAF E89-12 shown in Fig. 29.8 [Bo98], along with results of the previous SLAC experiments NE8 and NE17, in addition to other measurements at lower photon (γ -ray) energy, E_γ . In the CEBAF experiment the electron beam strikes a target producing a beam of γ -rays which are used for the investigation of the quark structure of nucleons and nuclei. In E89-12 the photon strikes a deuterium nucleus, ^2_1H which consists of a bound proton and neutron, causing it to dissociate into a proton and a neutron. The SLAC experiment presented some evidence that this dissociation gave indications that QCD effects (the presence of sub-structure in the nucleons) played a role, because the observed reaction obeyed what are called simple constituent quark-

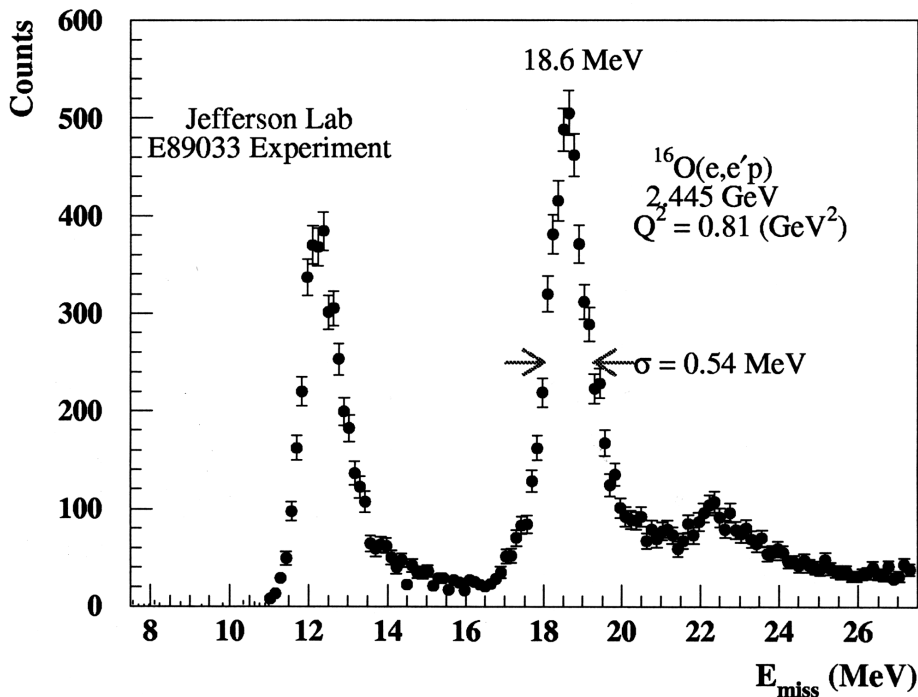


Fig. 29.7. Missing-mass spectrum in coincidence reaction $^{16}\text{O}(e, e' p)^{15}\text{N}^*$ taken at CEBAF at an incident electron energy of 2.445 GeV and four-momentum transfer squared of $0.81 (\text{GeV}/c)^2$. The first peak is the $(1p_{1/2})_{\pi}^{-1}$ proton hole in ^{16}O and the second the $(1p_{3/2})_{\pi}^{-1}$. Note the overall energy resolution in ^{15}N of $\Delta E/E = 0.54/2445 = 2.2 \times 10^{-4}$ [Ma00a]. The author would like to thank C. Perdrisat and K. Wijesooriya for the preparation of this figure.

counting rules at high energy. This behavior is signaled by the fact that the appropriately energy weighted cross section “scales”. So that, in this case, the product of the eleventh power of the square of the total energy in the center-of-momentum frame and the cross section becomes constant (see Fig. 29.8). The new CEBAF data exhibit a flat scaling behavior consistent with this rule, in photon energy approximately 1 to 4 GeV at a reaction angle of 90° (between the incident photon beam and the detected proton) for the $^2_1\text{H}(\gamma, p)n$ reaction. Furthermore, the new data also suggest that there is an onset of the scaling behavior above an energy of 3 GeV at a reaction angle of 37° . The results are consistent with an onset of scaling occurring at a transverse momentum of $1 \text{GeV } c^{-1}$. The new data support the picture where six constituent quarks in the deuteron (each nucleon contains three constituent quarks)

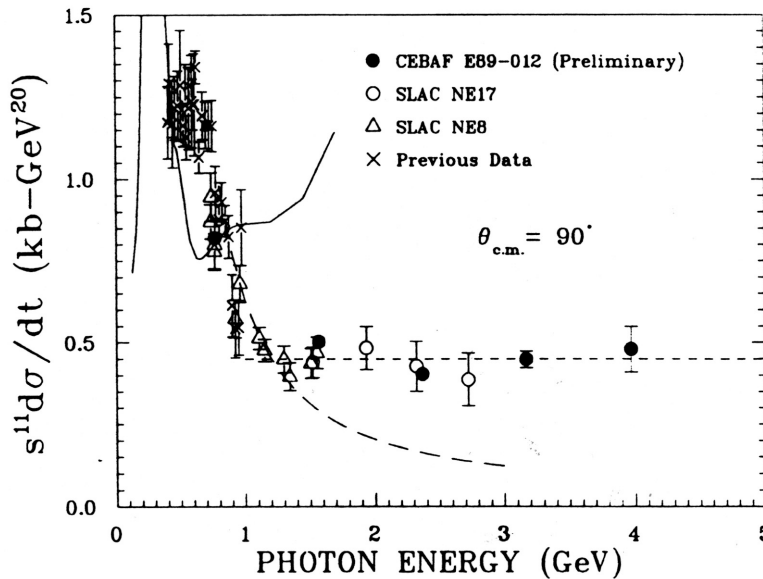


Fig. 29.8. The product of s (square of total $C - M$ energy)¹¹ times cross section at 90° in ${}^2_1\text{H}(\gamma, p)n$ as a function of photon energy in measurements in E89-12 at CEBAF [Bo98]. The short dashed curve is the predicted flat scaling behavior from a simple constituent quark counting rule. Also shown are data from the previous NE8 and NE17 experiments at SLAC, as well as data from lower energy.

organize a concerted response involving the exchange of gluons among themselves.²

The author served as Scientific Director of CEBAF from 1986 to 1992 when the initial scientific program and design for the initial complement of equipment were established.³ The reader is referred to an article which the author wrote for the publication *Physics News* in 1996 when the initial experimental results from that Laboratory appeared [Wa97]. Current information about the facilities and program at TJNAF can always be found on its website [TJ00].

² At least five gluon exchanges are required to reorganize the six quarks into two high-momentum outgoing nucleons. At very large s , the quark propagators each scale as $1/s$. The square of the amplitude, and conversion from solid angle to four-momentum transfer, then gives $d\sigma/dt \propto 1/s^{11}$.

³ John Domingo, Associate Director for Physics, led the equipment design and construction effort (see [Do93a]).